A **Examples of cell survival and death by flow cytometry**

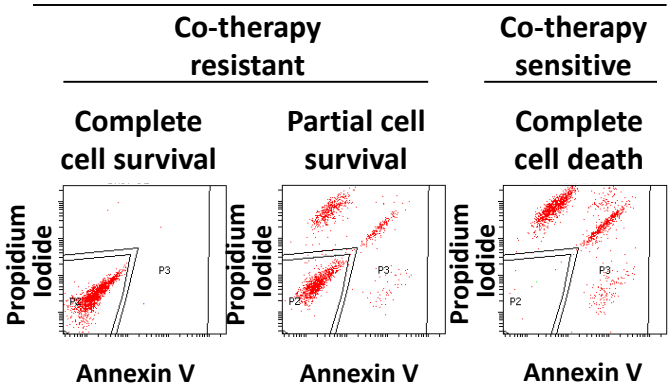

B **Examples of growth after re-plating without drug**

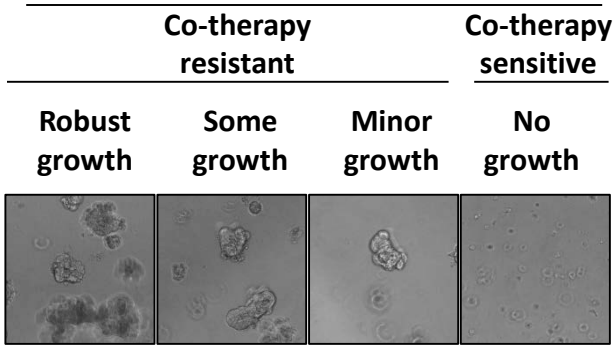

C **Pre-therapy Abdominal washings**

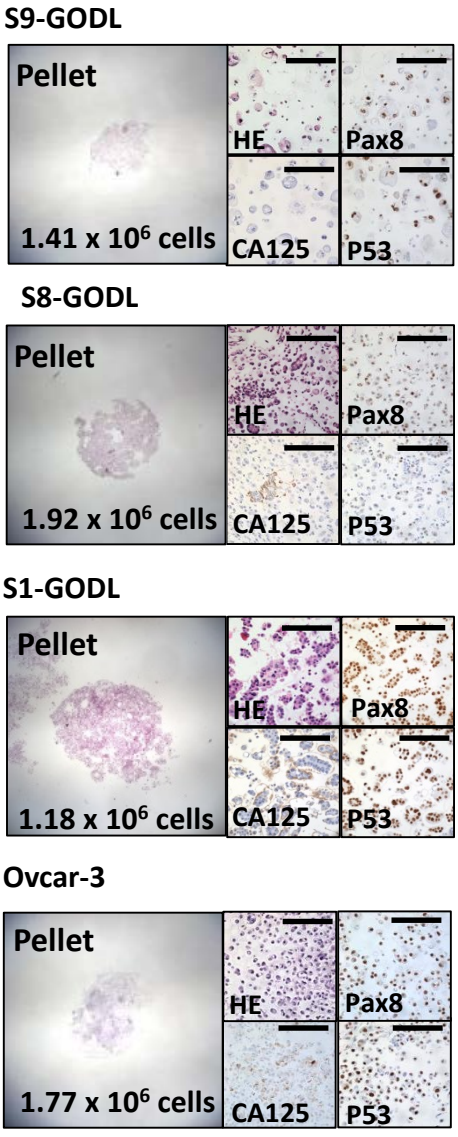

D **Drug levels detected in serum of treated mice**

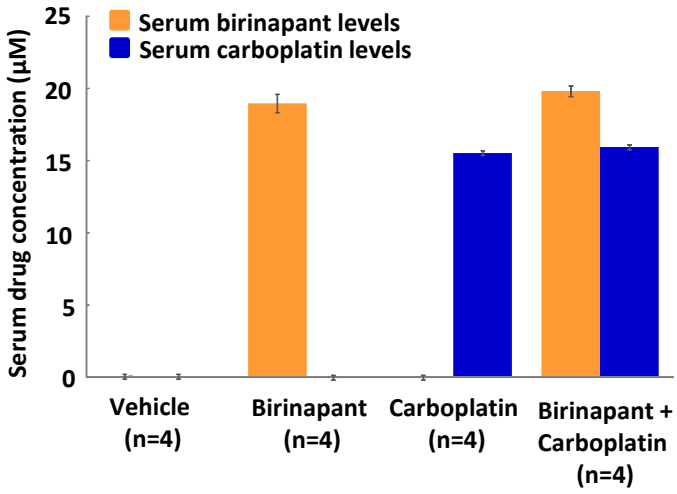

Supplementary Figure S1. In vitro drug response, in vivo tumor establishment and drug levels. A. Representative images used to assess cell survival by flow cytometry after drug treatment in the in vitro organoid bioassay. Samples where >1% of cell survived were designated as co-therapy resistant (two examples shown). **B.** Tumor cells from the in vitro organoid bioassay were re-plated without drug. If any in vitro growth of organoids was detected, samples were designated as co-therapy resistant. **C.** One mouse from each experimental cohort of the in vivo survival assay was euthanized prior to the start of therapy to confirm that tumors had established. The presence or absence of HGSC tumor cells in the abdominal washings of euthanized mice was verified by immunostaining for CA125, PAX8, and P53. Results confirm tumor take in mice from all four cohorts: S9-GODL, S8-GODL, S1-GODL and Ovcar-3. **D.** Birinapant, carboplatin, or both carboplatin and birinapant were detected in cohorts of mice treated with birinapant monotherapy, carboplatin monotherapy or birinapant and carboplatin co-therapy respectively 30 min after injection. Results are mean ± SE.

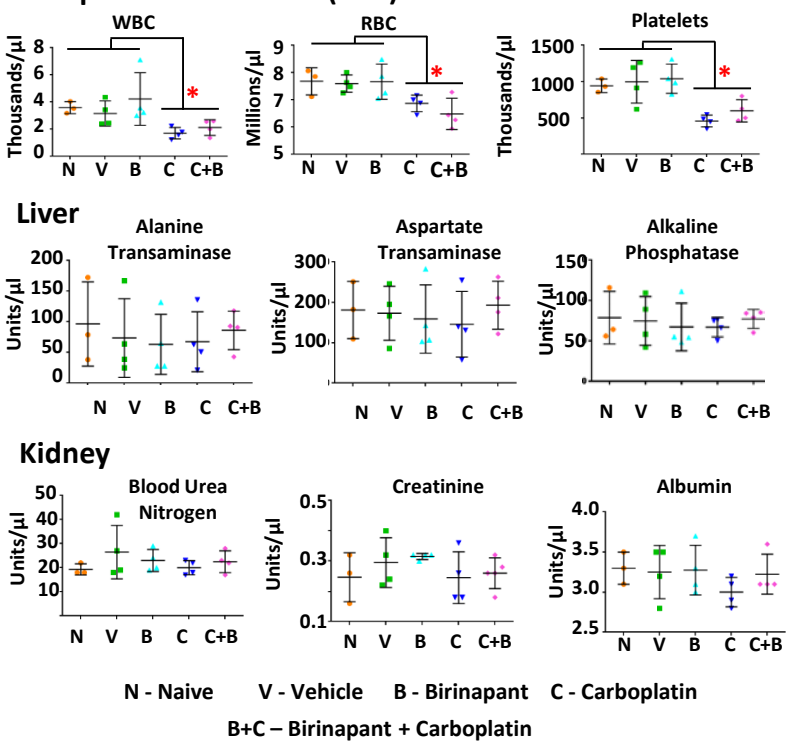

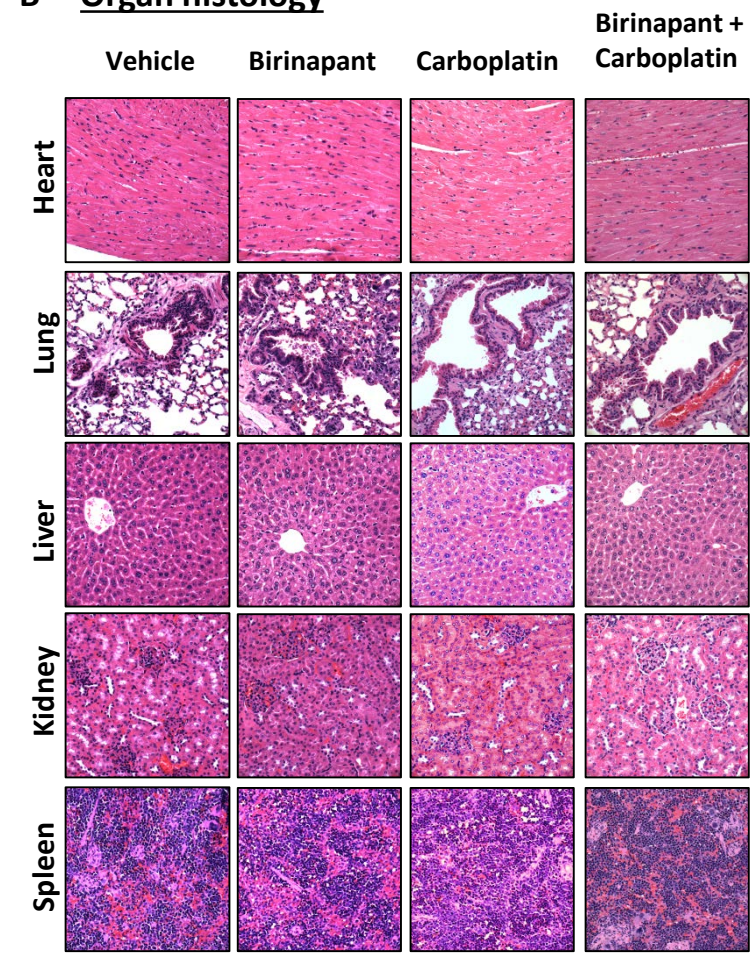

Supplementary Figure S2. Adding birinapant to carboplatin did not cause increased toxicity compared to carboplatin alone. A. A complete blood count (CBC) with differential and blood chemistry analysis was performed on naive NSG mice (n=3) and survival study mice (S8-, and S9-GODL) mice treated with vehicle (n=4), birinapant (n=4), carboplatin (n=4) or the combination of carboplatin and birinapant (n=4). The addition of birinapant to carboplatin did not cause additional hematologic toxicity compared to carboplatin. But CBC in both groups (carboplatin, carboplatin + birinapant) were statistically different compared to naïve, vehicle treated or birinapant treated mice (*). No significant differences in liver or kidney function was found between treatment groups based on blood chemistry analysis. Results are mean ± SE. **B.** No obvious signs of organ damage was found in any treatment group (n=2 per cohort, organs examined were HGSC tumor free sites of heart, lung, liver, kidney or spleen).

A **Reason for euthanasia in carboplatin vs birinapant + carboplatin treated mice**

Supplementary Fig. S3

Treatment	Reason for Euthanasia	Tumor in abdominal wash	Survival Interval (days off therapy until end point)	Age (days)
C	Hunched posture	yes	134	274
C	Ascites	yes	139	279
C	Abdominal bleeding	yes	141	281
C	Abdominal bleeding	yes	150	290
C	Abdominal bleeding	yes	150	290
C	Hunched posture	yes	156	296
C	Abdominal bleeding	yes	157	297
C	Abdominal bleeding	yes	174	314
B+C	Labored breathing	yes	240	380
B+C	Uterine prolapse	no	316	456
B+C	Abdominal bleeding	no	340	480
B+C	Distended abdomen	no	345	485
B+C	Eye infection	no	390	530

C – carboplatin treatment arm
B+C – birinapant and carboplatin co-therapy arm

B

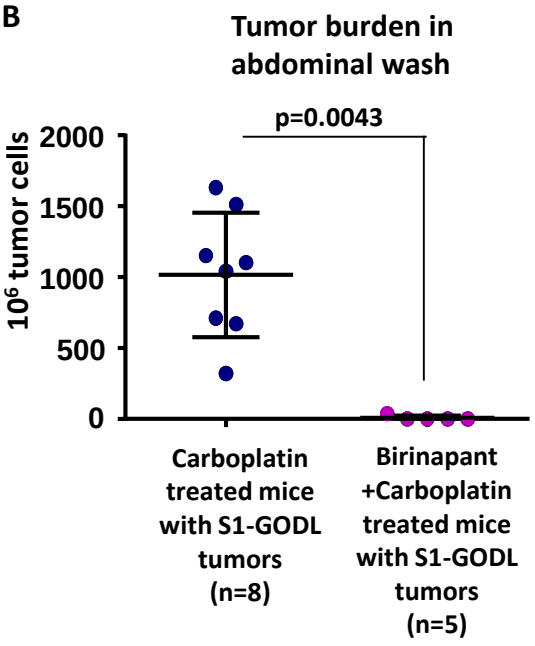

C

Treatment Group	Number of HGSC tumor implants detected on organs of mice bearing S1-GODL tumors after treatment with carboplatin vs co-therapy								
	Uterus	Fat Pad	Kidney	Lung	Liver	Spleen	Pancreas	Heart	Peritoneum
C	5	12	2	6	4	4	11	2	7
C	3	23	0	29	6	5	21	1	21
C	6	6	4	19	7	17	4	2	13
C	5	6	4	13	7	22	10	1	2
C	12	10	8	28	5	5	29	5	13
C	8	8	6	5	8	14	5	0	2
C	10	20	2	19	1	25	4	1	7
C	5	17	4	18	12	7	20	1	22
B+C	5	6	8	19	3	5	10	1	12
B+C	0	0	0	0	0	0	0	0	0
B+C	0	0	1	0	0	0	0	0	0
B+C	0	0	0	0	0	0	0	0	0
B+C	0	0	0	0	0	0	0	0	0

C – carboplatin treatment arm
B+C – birinapant and carboplatin co-therapy arm

Supplementary Figure S3. Cause of euthanasia in the vast majority of S1-GODL co-therapy treated mice was not HGSC tumor. A. Reasons for euthanasia of mice in the S1-GODL cohort treated with carboplatin or carboplatin and birinapant co-therapy. **B.** Majority (4/5) euthanized co-therapy treated mice in the S1-GODL cohort had no obvious HGSC burden in the abdomen based on histologic analysis of a pellet generated from an abdominal wash (immediately after euthanasia). One mouse in this cohort was found to have some disease in the abdominal wash. All carboplatin treated mice had large disease burden in their abdominal wash which was significantly greater compared to the co-therapy treated cohort (p=0.0043). Tumor cells were identified based on immunostaining for P53. **C.** Histologic sections of organs harvested from these euthanized mice were scored for disease based on presence of tumor foci staining positive for P53. In agreement with findings in the abdominal wash, 4/5 co-therapy treated mice had no obvious HGSC disease on organs analyzed. All carboplatin treated mice had obvious disease. Surviving mice in the S1-GODL cohort (n=3, age >640 days) have exceeded the median life span of NSG mice which is approximately 623 days. All S9-GODL co-therapy treated mice were still surviving (n=8, age >390 days). Upon histologic examination of organs, evidence of lymphosarcoma was found in two birinapant + carboplatin treated S1-GODL mice and two birinapant treated S1-GODL mice. Lymphomas have been observed in non-obese diabetic, scid, interleukin-2 receptor gamma null mice (Kato et al. Laboratory Animals 2009; **43:**402-404). Lymphosarcomas were not observed in any other cohort.

Figure supplement S4

Experimental Schema

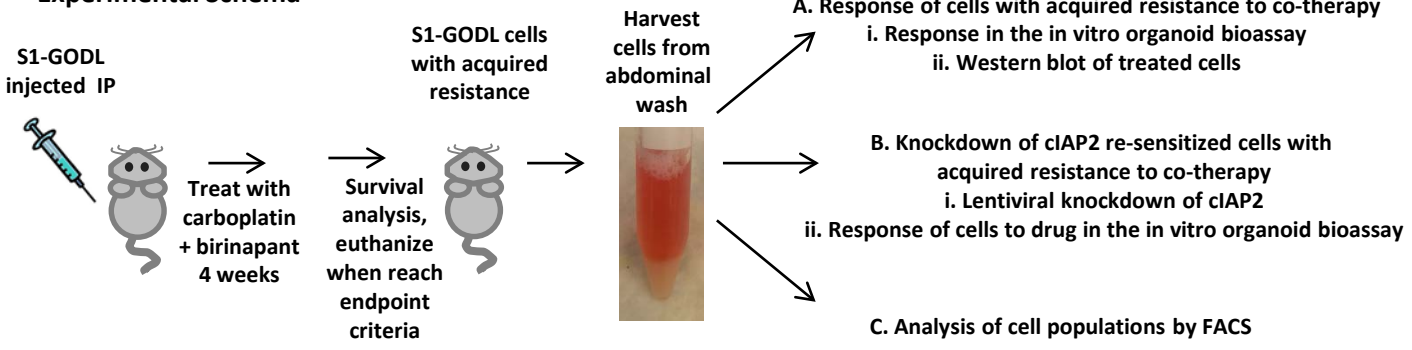

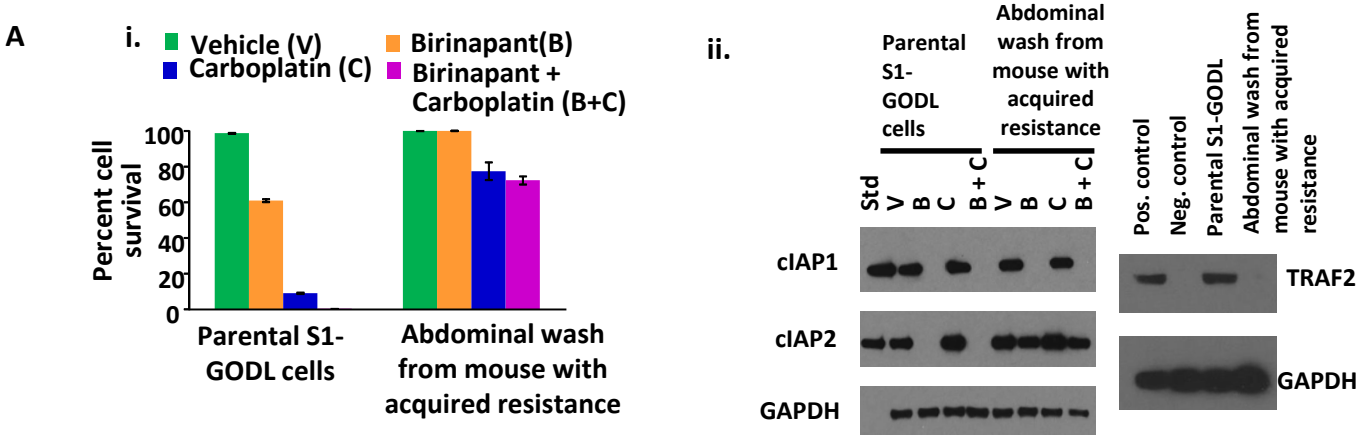

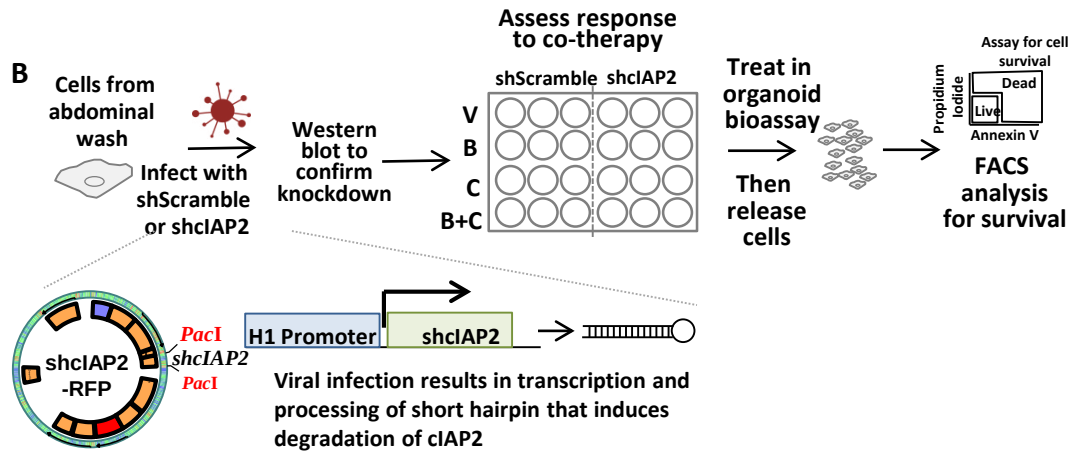

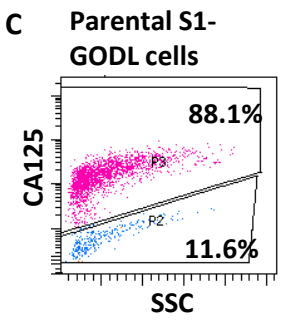

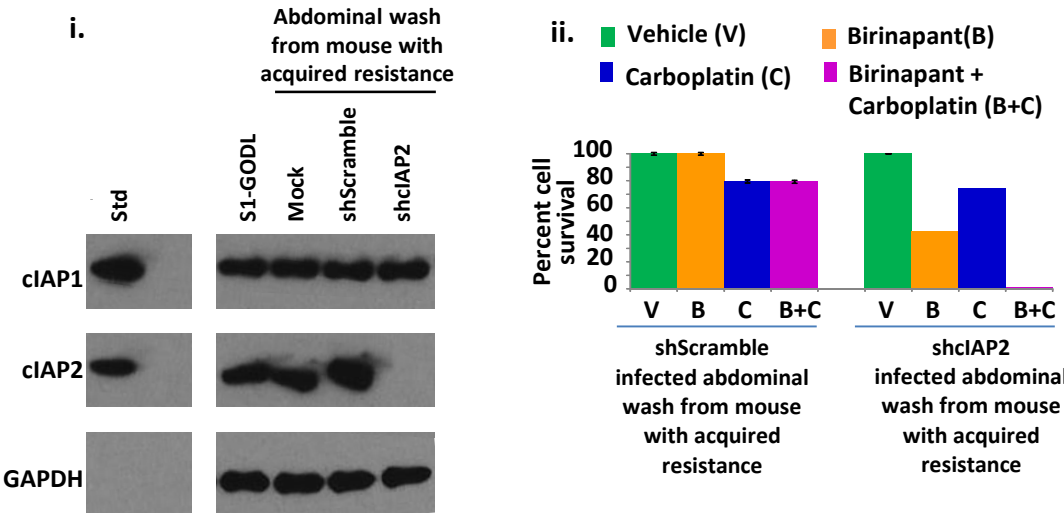

Supplementary Figure S4. The only S1-GODL co-therapy treated mouse with evidence of HGSC had a tumor with acquired resistance to birinapant. A. (i) Parental S1-GODL cells and cells harvested from the abdominal wash of the co-therapy treated mouse with tumor burden were analyzed in the in vitro organoid bioassay. While parental S1-GODL cells remained sensitive to co-therapy, cells in the abdominal wash of the co-therapy treated mouse demonstrated a resistant phenotype. The response of these cells to birinapant or carboplatin monotherapy was also diminished. Results are mean ± SD. **(ii)** The cells from the in vitro organoid bioassay were lysed and run on a Western blot with 20 ng of recombinant cIAP1 or cIAP2 (positive control). GAPDH was used as a loading control. Birinapant treatment resulted in degradation of cIAP1 but not cIAP2 in the cells from the abdominal wash of the mouse with acquired resistance. Levels of Traf2 protein were also diminished in the tumor cells with acquired resistance. No mutations in the cIAP2 or Traf2 gene were detected by direct sequencing of the Traf2 or cIAP2 transcripts. **B. (i)** To determine if the resistance to co-therapy likely arises from acquired resistance to birinapant and not carboplatin, cIAP2 expression was knocked down using a lentiviral construct expressing a short hairpin RNA targeting cIAP2. A lentivirus expressing the scrambled RNA sequence was used as a control. **(ii)** Knockdown of cIAP2 restored sensitivity to birinapant and co-therapy. In contrast, mock infected or scrambled control shRNA infected cells remained resistant. Results are mean ± SD. **C.** A greater proportion of tumor cells from the mouse with acquired resistance were CA125 negative compared to parental S1-GODL lines, likely accounting for a decreased response to carboplatin therapy.

A

In vitro growth of previously treated then passaged cells

Sample	Treatment			
	V	B	C	B+C
1	++	++	+	-
2	+++	++	+	-
3	++	+/++	+	-
4	++	+	+	-
5	++	++	+	-
6	+++	++	+	-
7	+++	++	+	-
8	+++	++	+	-
9	++	+/++	+	-
10	+++	++	+	-
11	+++	++	+	-
12	+++	++	+	-
13	+++	++	++	-/+
14	+++	+++	++	++
15	++	++	+	+
16	+++	+++	+	+
17	++	+	+	+
18	+++	+++	+	+
19	+++	++/+++	++	++
20	+++	+++	++	++
21	+++	++	++	++
22	+++	++	++	++
23	++	++	+/++	+/++

Blue text – specimen was co-therapy sensitive in the in vitro organoid bioassay
Pink text – specimen was co-therapy resistant in the in vitro organoid bioassay

B Mutation of cIAP is uncommon in HGSC

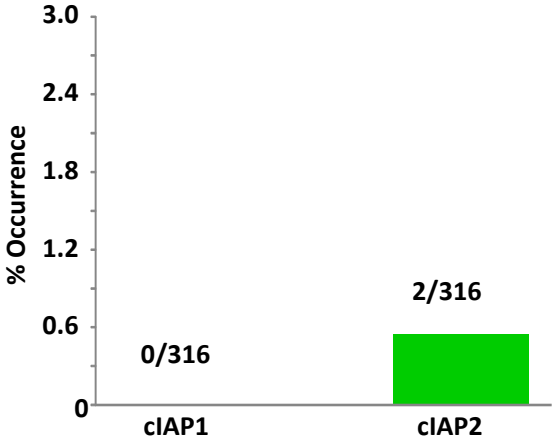

Extracted from TCGA Database of High grade serous ovarian cancer

Nature. 2011;474(7353):609-15.

Supplementary Figure S5. Birinapant and carboplatin co-therapy prevents re-growth of HGSC cells after the cessation of treatment. A. After 72 hours, cells treated in the in vitro organoid bioassay were dissociated and re-plated without drug. Organoid growth was scored after 7 days. HGSC samples sensitive to co-therapy showed no growth 7 days after re-plating. In contrast, HGSCs classified as co-therapy resistant demonstrated growth in this assay. Growth was seen in all vehicle or monotherapy treated cells. **B.** The mutational status of cIAP genes was examined in a panel of 316 HGSCs in the Cancer Genome Atlas database (The Cancer Genome Atlas Research Network. Nature 2011 **474**:609-615.). No mutations were reported in the cIAP1 gene, and only 2 mutations in 316 cases (S248C or T536R) were reported in cIAP2.

Supplementary Fig. S6

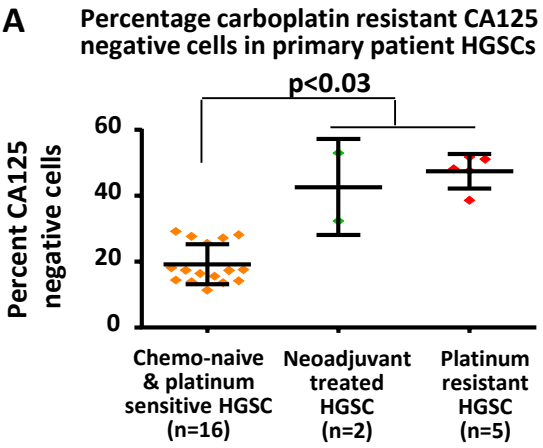

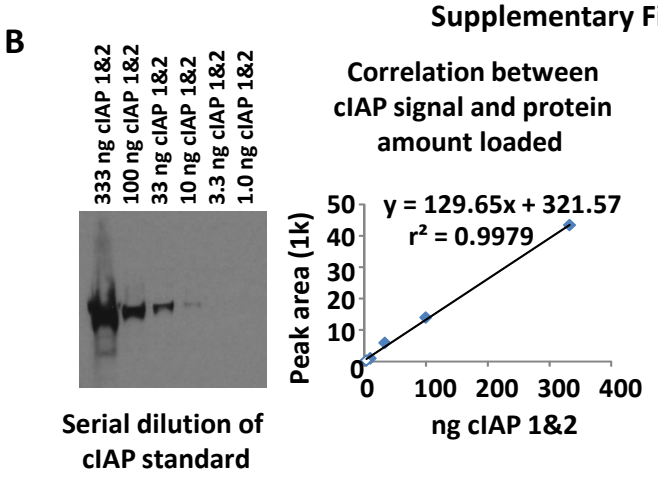

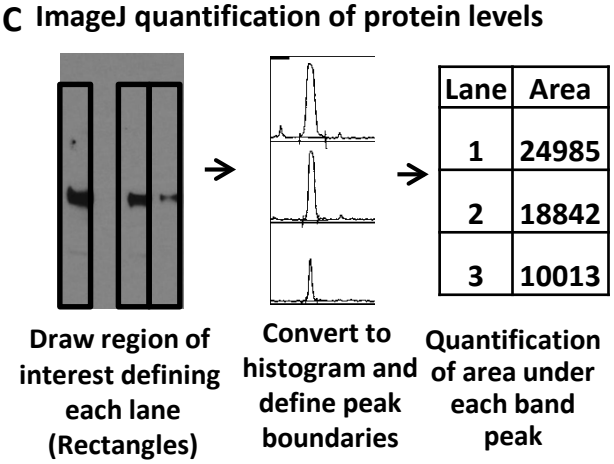

D Example calculations

GAPDH sample	GAPDH pixel area	Normalization Factor (N_i)	cIAP sample	cIAP pixel area	Normalized cIAP (C_i)	cIAP Expression (ng cIAP)
	GAPDH	$N_i = GAPDH_i / GAPDH_{max}$		cIAP	$C_i = cIAP_i / N_i$	ng $cIAP_i = [C_i/C_{Std}]$ x 40ng
Std	N/A	N/A	Std	37658.3	37658.3	40
Pt. 6 125-	33293.9	0.96827	Pt. 6 125-	25270.7	26098.6	27.72
Pt. 6 125+	33115.3	0.96308	Pt. 6 125+	8282.0	8599.5	9.13
Pt. 4 125-	34384.7	1.00000	Pt. 4 125-	33783.1	33783.1	35.88
Pt. 4 125+	34075.8	0.99102	Pt. 4 125+	13094.5	13213.2	14.03

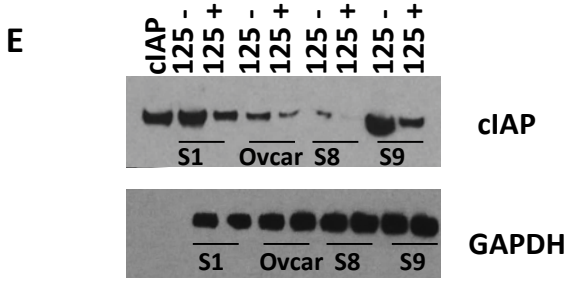

Cell line	ng cIAP in 20 µg of lysate	Above or below threshold midpoint (26.1 ng)	Response to co-therapy in vivo
S9-GODL	52.1	Above	Co-therapy sensitive
S1-GODL	64.0	Above	Co-therapy sensitive
S8-GODL	3.5	Below	Co-therapy resistant
Ovcar-3	21.5	Below	Co-therapy resistant

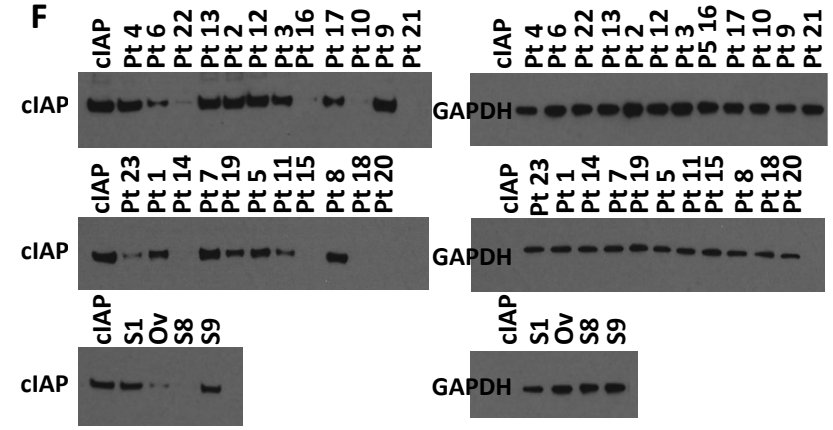

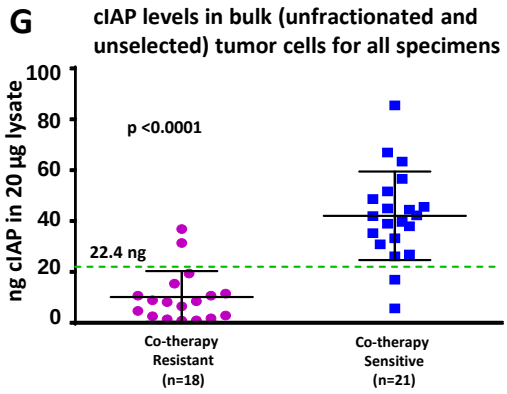

Supplementary Figure S6. Percentages of platinum resistant HGSC tumor cells and methodology for quantification of cIAP. A. The percentage of CA125 negative cells was significantly higher (2-fold) in clinically-defined platinum resistant (n=5) and neoadjuvant treated (n=2) disease compared to chemo-naïve and recurrent platinum sensitive (n=16) HGSCs ($p<0.03$)**. B.** Pan-cIAP standards, containing equal amounts of cIAP1 and cIAP2, were run in serial three-fold dilutions and analyzed by western blot. A representative blot is shown. Quantification of cIAP levels measured by Image J was linear ($r^2 = 0.9979$). **C.** Workflow for the analysis of cIAP levels using ImageJ software. Lanes were defined using the region of interest tool of ImageJ. Histograms were produced from each lane and peak boundaries in each histogram were manually defined. The pixel area under the curve was then analyzed for each peak and used to compare protein expression. **D.** Example calculations for quantification of cIAP are shown for two specimens. Cell lysates were normalized based on GAPDH signal. The lane with the highest GAPDH signal in each blot ($GAPDH_{max}$) was identified. GAPDH signal for each lysate ($GAPDH_i$) was normalized to $GAPDH_{max}$ using the following formula $N_i=GAPDH_i/GAPDH_{max}$ to yield a normalization factor (N_i). This factor was used to normalize the cIAP signal in each lysate (C_i=cIAP peak area per lysate/N_i). To quantify amount of cIAP per lane each lysate was then compared to a cIAP standard. To achieve this goal each blot included 40 ng cIAP standard (20 ng each of cIAP1 and cIAP2). The peak area of cIAP standard per blot was measured and called $C_{std.}$ Total cIAP amount of each lysate was then calculated by dividing normalized cIAP (C_i) by the cIAP standard and multiplying by 40ng (ng $cIAP_i$ = $[C_i/C_{std}]$ x 40ng). **E.** Using the threshold midpoint of 26.1ng cIAP per 20µg of CA125 negative cell lysate (determined from analysis of the 23 clinical samples, Fig. 3b), co-therapy sensitive vs co-therapy resistant HGSC cell lines were accurately segregated. **F.** Western blots of cIAP expression in unfractionated (bulk) HGSC cells are shown. **G.** Levels of cIAP were plotted in bulk primary HGSC clinical specimens, HGSC and non-HGSC cell lines (unfractionated HGSCs and vehicle treated non-HGSC cell lines) categorized as co-therapy sensitive vs. resistant. cIAP expression here could segregate co-therapy sensitive vs resistant specimens using a threshold midpoint of 22.4ng cIAP in 20µg of tumor lysate; however, accuracy was diminished (89.7% here) compared to 100% when cIAP expression was quantified in the platinum resistant enriched cell populations.

Supplementary Fig. S7

A

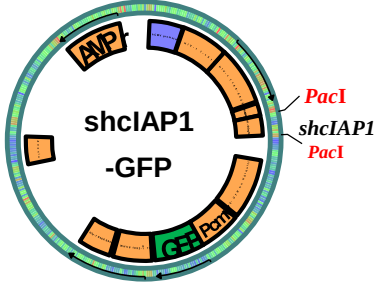

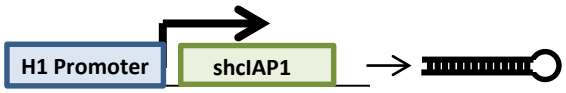

Viral infection results in transcription and processing of short hairpin that induces degradation of cIAP1

B

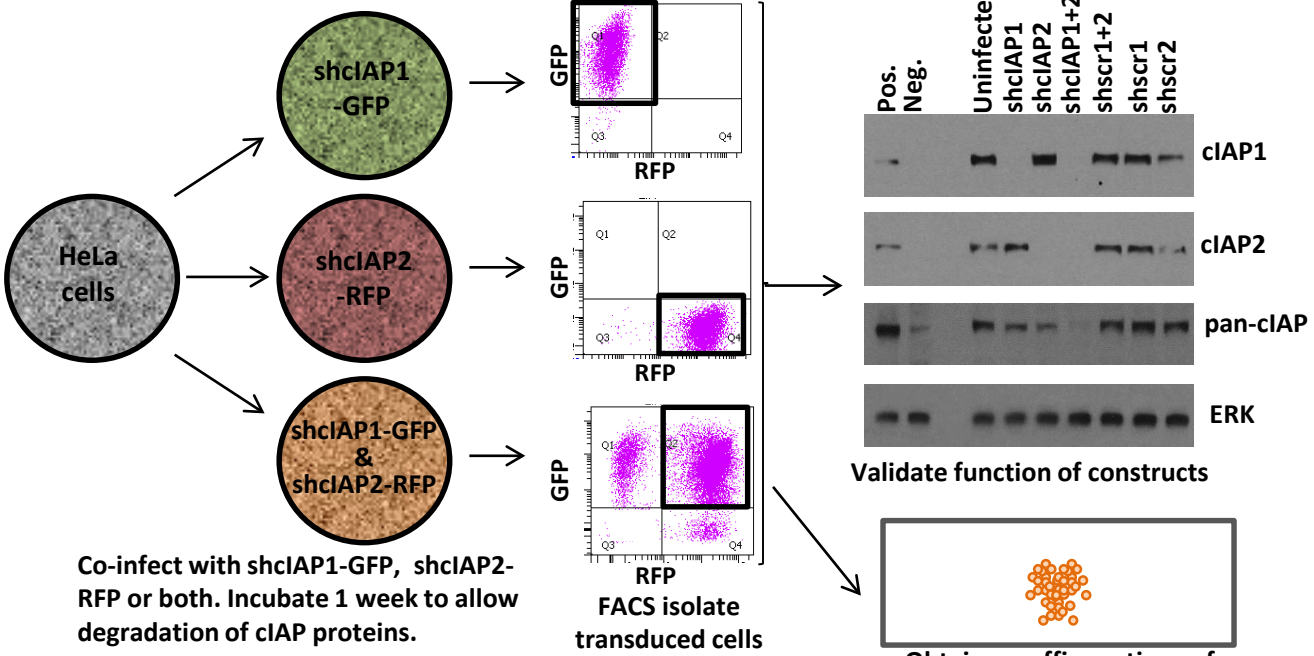

Co-infect with shcIAP1-GFP, shcIAP2-RFP or both. Incubate 1 week to allow degradation of cIAP proteins.

FACS isolate transduced cells

Validate function of constructs

Obtain paraffin sections of infected Hela cells for IHC control

C

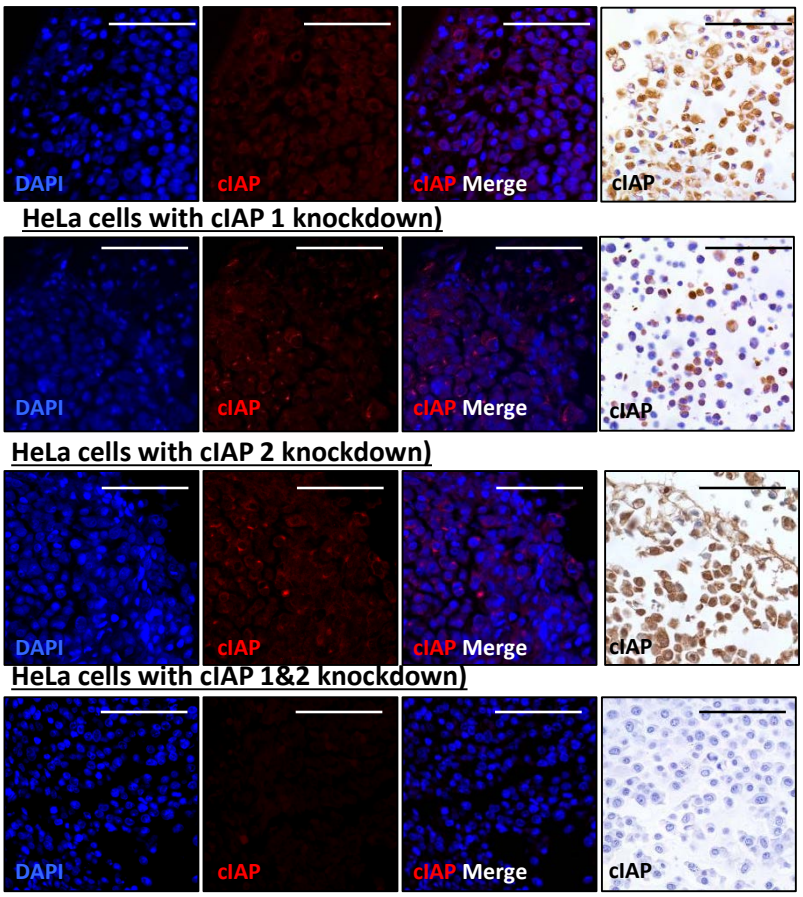

Supplementary Figure S7. Testing specificity of the pan-cIAP antibody in detecting both cIAP1 and cIAP2 by immunohistochemistry. A. Color-tagged lentiviral knockdown vectors expressing short hairpin RNAs specifically targeting cIAP1 (shown here) or cIAP2 (Fig. S4B) were constructed to test the specificity of commercially available pan-cIAP antibodies. **B.** HeLa cells were infected with lentiviruses to knockdown cIAP1, cIAP2, or both cIAP1&2 simultaneously. Efficacy of knockdown with these vectors was assessed by western blot in cells isolated by fluorescence-activated cell sorting. Aliquots of isolated cells was used to produce formalin-fixed paraffin-embedded control slides. **C.** Immunostaining of uninfected HeLa cells or HeLa cells infected with one or both knock down vectors demonstrate that the pan-cIAP antibody detects both cIAP1 and cIAP2. Examples of individual channels, merged images and DAB (3'3'-diaminobenzine) staining are shown. Scale bars equal 100µm.

Supplementary Fig. S8

A Platinum resistant, co-therapy sensitive HGSC

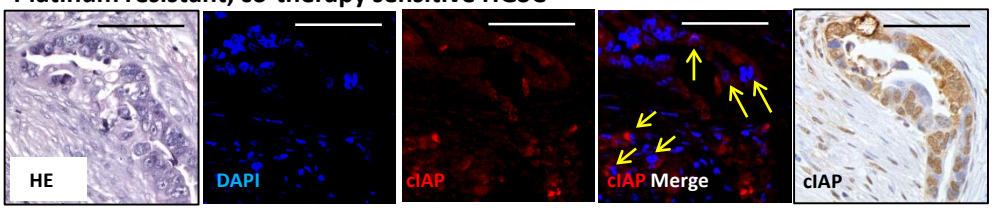

Platinum resistant, co-therapy resistant HGSC

B HGSC cell lines

S8-GODL
(Platinum resistant, co-therapy resistant)

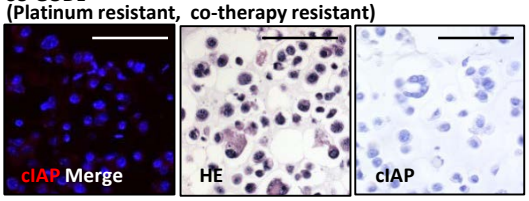

S9-GODL
(Platinum resistant, co-therapy sensitive)

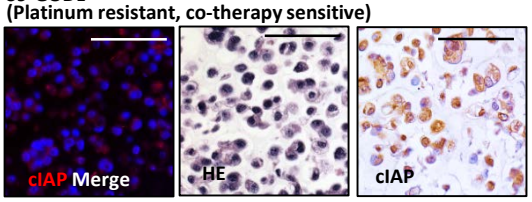

Non-HGSC cell lines

DLD-1
(Platinum resistant, co-therapy resistant)

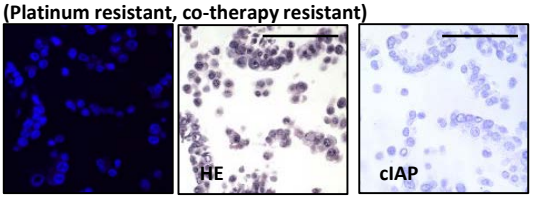

Colo1
(Platinum resistant, co-therapy sensitive)

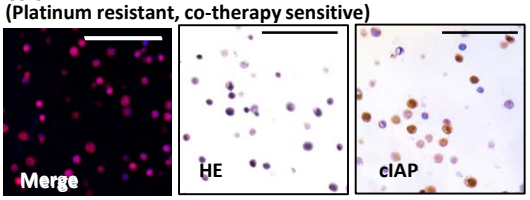

C Quantification of cIAP by IHC identifies co-therapy sensitive specimens

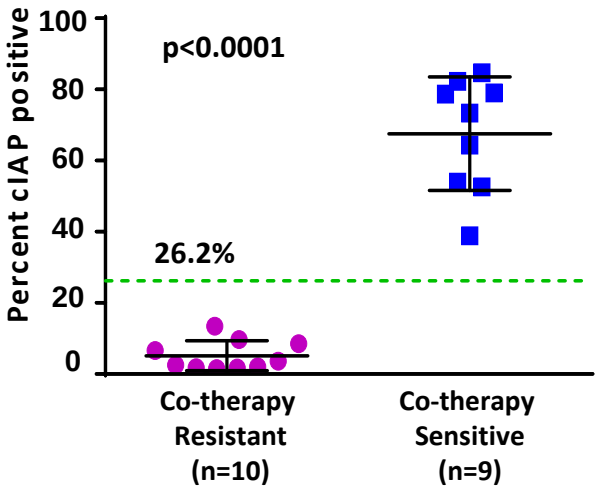

Supplementary Figure S8. Percentage of cIAP positive cells detected by immunohistochemistry may segregate platinum resistant co-therapy sensitive vs. resistant HGSCs. A. Immunostaining of platinum resistant, co-therapy sensitive HGSCs demonstrate robust cIAP expression. In contrast, platinum resistant, co-therapy resistant HGSCs had low expression of cIAP. Representative images are shown. Hematoxylin and eosin staining (HE), individual channels and the merged image for immunoflurorescence are shown. Yellow arrows indicate cIAP positive cells. Immunostaining using DAB (3'3'-diaminobenzine) detection yielded similar results. Scale bars equal 100µm. **B.** Images were taken of the platinum resistant HGSC and non-HGSC cell line pellets stained for cIAP. A high percentage of cells expressed cIAP in co-therapy sensitive cell lines. Conversely, co-therapy resistant cell lines had low cIAP expression. HE, merged and DAB stained image examples are shown for HGSC and non-HGSC cell lines. Representative images are shown here. Scale bars equal 100µm. **C.** Percentage of cIAP cells (number of cIAP positive cells/number of total cells) in platinum resistant carcinomas and platinum resistant cell lines were plotted based on response to co-therapy (sensitive vs resistant). A threshold midpoint of 26.2% cIAP positive cells (threshold range 13.5% – 38.9%) accurately segregated the co-therapy sensitive from resistant samples ($p<0.0001$).

Table S1: Median survival broken down by treatment category

Cell line	Treatment Arm	Median Cohort Survival (days)	95% Confidence Interval (days)
S9-GODL	Vehicle	72.0	61.0-74.0
	Birinapant	70.0	61.0-96.0
	Carboplatin	67.5	62.0-75.0
	Co-therapy	>240	ND*
S8-GODL	Vehicle	93.5	82.0-103.0
	Birinapant	101.5	54.0-109.0
	Carboplatin	92.5	86.0-102.0
	Co-therapy	105.0	92.0-117.0
S1-GODL	Vehicle	94.5	74.0-106.0
	Birinapant	94.5	74.0-106.0
	Carboplatin	150.0	134.0-157.0
	Co-therapy	367.5	240.0-ND*
Ovcar-3	Vehicle	85.5	74.0-95.0
	Birinapant	97.0	67.0-101.0
	Carboplatin	121.0	105-132.0
	Co-therapy	127.0	117.0-145.0

Co-therapy denotes treatment with birinapant + carboplatin

* N.D. – not determined

Table S2: Pairwise comparisons of survival outcomes by treatment group

cell line	treatment group 1	vs	treatment group 2	adjusted p value
S9-GODL	Vehicle	vs	Birinapant	0.8013
	Vehicle	vs	Carboplatin	0.9082
	Vehicle	vs	Co-therapy	< 0.0001
	Birinapant	vs	Carboplatin	0.7127
	Birinapant	vs	Co-therapy	0.0002
	Carboplatin	vs	Co-therapy	< 0.0001
S8-GODL	Vehicle	vs	Birinapant	0.2525
	Vehicle	vs	Carboplatin	0.9207
	Vehicle	vs	Co-therapy	0.0963
	Birinapant	vs	Carboplatin	0.2101
	Birinapant	vs	Co-therapy	0.6037
	Carboplatin	vs	Co-therapy	0.0753
S1-GODL	Vehicle	vs	Birinapant	0.9585
	Vehicle	vs	Carboplatin	0.0734
	Vehicle	vs	Co-therapy	< 0.0001
	Birinapant	vs	Carboplatin	0.0659
	Birinapant	vs	Co-therapy	< 0.0001
	Carboplatin	vs	Co-therapy	0.0100
Ovcar-3	Vehicle	vs	Birinapant	0.5048
	Vehicle	vs	Carboplatin	0.0068
	Vehicle	vs	Co-therapy	< 0.0001
	Birinapant	vs	Carboplatin	0.0324
	Birinapant	vs	Co-therapy	< 0.0001
	Carboplatin	vs	Co-therapy	0.2340

Co-therapy denotes treatment with birinapant + carboplatin

Table S3: Clinical information associated with human HGSC specimens used in this study

Patient Number	Age	Diagnosis	Chemonaive or Recurrent	Platinum sensitivity	Co-therapy sensitivity
1	55	Stage IIIC HGSC	Chemonaive	Sensitive	Sensitive
2	61	Stage IIIC HGSC	Chemonaive	Sensitive	Sensitive
3	49	Stage IIIC HGSC	Chemonaive	Sensitive	Sensitive
4	41	Stage IIIC HGSC	Chemonaive	Sensitive	Sensitive
5	72	Stage IIIC HGSC	Chemonaive	Sensitive	Sensitive
6	74	Stage IIIC HGSC	Chemonaive	Sensitive	Sensitive
7	31	Stage IV HGSC	Chemonaive	Sensitive	Sensitive
8	58	Stage IIIC HGSC	Recurrent	Sensitive	Sensitive
9	64	Stage IVB HGSC	Chemonaive	Sensitive	Sensitive
10	76	Stage IV HGSC	Chemonaive	Sensitive	Sensitive
11	50	Stage IIIC HGSC	Chemonaive	Sensitive	Sensitive
12	72	Stage IIIC HGSC	Recurrent	Resistant	Sensitive
13	56	Stage IIIC HGSC	Recurrent	Resistant	Sensitive
14	61	Stage IA HGSC	Chemonaive	Sensitive	Resistant
15	56	Stage IIIC HGSC	Chemonaive	Sensitive	Resistant
16	61	Stage IIIC HGSC	Chemonaive	Sensitive	Resistant
17	60	Stage IIIC HGSC	Chemonaive	Sensitive	Resistant
18	63	Stage IIIC HGSC	Chemonaive	Sensitive	Resistant
19	63	Stage IIIC HGSC	Chemonaive	Neoadjuvant	Resistant
20	57	Stage IIIC HGSC	Chemonaive	Neoadjuvant	Resistant
21	59	Stage IIIC HGSC	Recurrent	Resistant	Resistant
22	70	Stage IIIC HGSC	Recurrent	Resistant	Resistant
23	59	Stage IV HGSC	Recurrent	Resistant	Resistant
24	71	Stage IIIC HGSC	Chemonaive	Sensitive	Resistant
25	45	Stage IIIC HGSC	Chemonaive	Sensitive	Sensitive
26	70	Stage IIIC HGSC	Chemonaive	Sensitive	Resistant

Table S4: Platinum resistant non-HGSC cancer cell lines tested for response to carboplatin and birinapant co-therapy

Cancer Type	Cell line	ATCC number	Classification
Cervical Cancer	HeLa	CCL-2	cervical adenocarcinoma
	SiHa	HTB-35	grade II squamous cell cervical carcinoma
	CaSki	CRL-1550	epidermoid carcinoma, metastatic to small intestine
Lung Cancer	A549	CCL-185	alveolar basal lung carcinoma
	H460	HTB-177	non-small cell lung cancer
	H226	CRL-5826	squamous cell carcinoma
Colorectal cancer	SW620	CCl-227	colorectal adenocarcinoma (Duke's type C), metastatic to lymph node
	Colo205	CCL-222	colorectal adenocarcinoma (Duke's type D)
	DLD-1	CCL-221	colorectal adenocarcinoma (Duke's type C)
Bladder Cancer	J82	HTB-1	transitional cell bladder carcinoma
	5637	HTB-9	grade II urinary bladder carcinoma
	HT1197	CRL-1473	urinary bladder carcinoma